Paleobiology

cambridge.org/pab

Quantifying the rise of animals during the Ediacaran–Cambrian using ichnodissimilarity

Zekun Wang[1], Imran A. Rahman[1,2] and Li-Jun Zhang[3]

[1]Natural History Museum, London SW7 5BD, U.K.
[2]Oxford University Museum of Natural History, University of Oxford, Oxford OX1 3PW, U.K.
[3]Institute of Resources and Environment, Collaborative Innovation Center of Coalbed Methane and Shale Gas for Central Plains Economic Region, Henan Polytechnic University, Jiaozuo, China

Featured Article

Cite this article: Wang Z, Rahman IA, Zhang L-J (2024). Quantifying the rise of animals during the Ediacaran–Cambrian using ichnodissimilarity. *Paleobiology* **50**, 532–547. https://doi.org/10.1017/pab.2024.40

Received: 5 February 2024
Revised: 14 August 2024
Accepted: 22 August 2024
First published online: 10 December 2024

Corresponding author:
Zekun Wang;
Email: zekun.wang@nhm.ac.uk

Non-technical Summary

The trace fossil record provides key insights into the evolution of early animals during the Ediacaran/Cambrian transition. By examining the diversity of these fossils, we can understand how early animal behaviors and body plans developed. We introduced a new mathematical method based on vectors to measure differences in trace fossil diversity. Using this method, we analyzed a large dataset of trace fossils and discovered the timings of important evolutionary events. Our findings show that early animals diversified in two stages and more quickly in shallow-marine environments and gradually specialized their ecological roles.

Abstract

The trace fossil record provides important insights into the evolution of early animals during the Ediacaran/Cambrian transition, with changes in ichnodiversity through time and between environments informing on the diversification of major body plans, behaviors, and niches. To quantify variation in the diversity of trace fossils across this critical interval, we propose a measure of trace fossil dissimilarity (ichnodissimilarity) based on vector calculation. Furthermore, by comparing discrepancies between the angular bisector and mean vector of two sets of vectorized fossil data, we are able to weigh the relative contribution of increases and decreases in the variation of occurrences of taxa. We used this metric to analyze an expansive dataset of Ediacaran/Cambrian trace fossils. The results allowed us to quantify the diversification of traces across this transition, informing on the timing of first appearance of different behaviors (e.g., foraging, grazing, and resting) and functional groups. By interpreting the results in the context of environmental changes and advancements in motility and sensory capabilities, we were able to pinpoint the onset and sequence of the Fortunian diversification event, Cambrian information revolution, and agronomic revolution, shedding light on the evolution of organismal body plans, behaviors, and locomotion during the Ediacaran/Cambrian transition. We identified two phases of origination and expansion during the divergence of early animal traces. Furthermore, by analyzing shallow- and deep-marine trace fossils, we were able to uncover evidence for a more rapid diversification of traces in shallow-marine environments, with progressive niche partitioning through the Ediacaran to Cambrian.

Introduction

The Ediacaran (~635–541 Ma) to Cambrian (~541–485 Ma) periods document critical steps in the earliest evolution of complex animal life. During this interval, almost all the major groups of modern animals appeared and diversified. This emergent phenomenon (Artime and De Domenico 2022) is thought to reflect complex nonlinear interactions between new macroscopic multicellular life-forms and the environment. However, the body fossil record from this time span (especially the Ediacaran) is patchy and depends on narrow preservational windows (Mángano and Buatois 2014), which handicaps study of this fundamental evolutionary radiation. Therefore, trace fossils provide an alternative and complementary record of how early animals interacted with their environments. Trace fossils are thought to document the first appearance of bilaterian animals (Gehling et al. 2014; Mángano and Buatois 2016; Chen et al. 2019), with some traces like *Cruziana* appearing earlier than their putative tracemakers (Antcliffe et al. 2014). Moreover, *Treptichnus pedum* marks the GSSP for the Ediacaran/Cambrian boundary (Buatois 2018). Consequently, the ichnological record can provide very valuable insights into ancient ecosystems and environments during this critical interval, informing on major changes in biodiversity (Buatois and Mángano 2018), including evolutionary radiations and extinctions (Mángano and Buatois 2016).

Among these evolutionary events, the divergence of metazoans across the Ediacaran and Cambrian is uniquely profound. It is believed that one of the important factors associated with the Cambrian explosion and the initial diversification of animal phyla is the fundamental

© The Author(s), 2024. Published by Cambridge University Press on behalf of Paleontological Society

change in the nature of the seafloor from Neoproterozoic-style substrates with microbial mats and limited bioturbation to Phanerozoic-style unconsolidated soft substrates with a well-developed mixed layer (Mángano and Buatois 2014, 2016). This shift in the complexity and heterogeneity of the substrate, termed the "agronomic revolution" (AR; Seilacher and Pflüger 1994), is believed to have had a significant impact on the evolution of motility and feeding behaviors in early animals (i.e., the Cambrian substrate revolution), driving them to develop new strategies for moving across and through the seafloor and locating and capturing food, some of which are recorded in the trace fossil record. Consequently, studying Ediacaran and Cambrian trace fossils can help elucidate the pattern and process of this major evolutionary episode. However, to accurately quantify the diversification of these early traces, an advanced mathematical tool that can effectively and precisely pinpoint changes in the ichnological record is first required.

A typical approach to quantifying the diversification of traces produced by different behaviors and tracemakers on various substrates is to examine ichnodiversity. This usually entails simply counting the number of ichnogenera that can be identified at a particular site (Mángano and Buatois 2016). However, this measure of alpha diversity may be inadequate when comparing the differences between two sites over an environmental gradient or through time. As a result, the concept of beta diversity (Whittaker 1960), which measures differences in diversity between sites, has also been used in ichnology (Mángano and Buatois 2016); in broader terms, beta diversity can be seen as a kind of dissimilarity. Although the dissimilarity of trace fossils (ichnodissimilarity) does not necessarily equate to differences in the diversity of the tracemakers, this measure can help us uncover how organism body plans and behaviors changed during major evolutionary radiations and mass extinction events. Ichnodissimilarity is therefore a potentially important tool for studying the early history of life.

Valuable though this metric is, quantitative definitions of dissimilarity are often simple and rough. The measure of beta diversity that is most commonly used in ichnology (Chao et al. 2005) is defined as:

$$\beta = (N_1 - S_{12}) + (N_2 - S_{12}), \quad (1)$$

where β is the beta diversity/dissimilarity, equivalent to the "absolute species turnover"; N_1 and N_2 are the total numbers of species (or genera) at site 1 and site 2, respectively; and S_{12} denotes the number of shared species (genera) between the two sites.

This definition is unnormalized and, to some extent, case dependent. It is therefore difficult to compare different studies/sites. Alternative definitions of beta diversity proposed by Whittaker (1960; Jost 2007) and McArthur et al. (1966) that are widely used in ecology do not rely on simply counting numbers of species, but instead depend on alpha and gamma diversity (Ricotta 2017) and are incapable of taking details of each observation into account (e.g., weighting by the number of each observation). These are sometimes termed "true" beta diversities (Beck et al. 2013). A third kind of measure is the pairwise dissimilarity calculated by comparing relative abundances species by species, such as the Horn overlap and the Morisita-Horn index (Horn 1966). However, these indexes cannot establish which species diversity is larger between the two observations, nor do they allow us to identify whether dissimilarity is caused by presence or absence of new/more species. Moreover, there is also a computational bias in the dissimilarity calculated by the Morisita-Horn index, which will be discussed later.

Orloci (1967) proposed a vector-based method to calculate the dissimilarity between two communities, wherein each element in the vector represents a species, and the length of the chord between the two vectors is used to define dissimilarity. The chord distance can be scaled within the range between 0 and 1 for easier interpretation (Conde and Domínguez 2018). Similarly, taking the cosine of the angle between the two vectors is another simple way of defining this measure (Cheeyham and Hazel 1969). However, there is a disadvantage in using this approach when calculating dissimilarity, because cosine does not obey the law of addition, which means it cannot be directly decomposed into components related to increase or decrease of taxa and their abundance.

Herein, we present an alternative measure of dissimilarity based on vector theory using the exact angle between two normalized vectors instead of cosines. By comparing discrepancies between the angular bisector and mean vector, we can weigh the relative importance of increases and decreases in the variation of taxonomic occurrences. We can therefore define a ratio between the split angles that describes the balance of turnovers, informing on the main driver underlying any obtained dissimilarities. We use this metric to quantify the evolution of benthic communities across the Ediacaran–Cambrian interval based on the trace fossil record. Traces representing typical functional groups (e.g., epifaunal bioturbators, surficial modifiers, regenerators, conveyors, and biodiffusors) and behaviors (e.g., agrichnia, domichnia, pascichnia, and repichnia) are studied, with their variation through time analyzed. The distribution and evolution of traces across environmental gradients are also investigated for this critical interval (Bottjer et al. 2000).

We first introduce the definition of our measure of dissimilarity, including both 1/0-based and probabilistic calculations, and propose the "balance index for occurrences" and the "balance index for origination and extinction." We then provide a comparison between the dissimilarity index and existing measures and undertake a convergence study. Finally, we apply the proposed metric to the trace fossil record in order to quantify the variance of behaviors and functional groups in response to environmental change during the Ediacaran and Cambrian periods.

Methods: Vector Calculation and Dissimilarity

Basic Formulation

If we assume there exists an extremely large vector that can house all species, with each species represented by a certain value, then this vector becomes a coordinate that can indicate the diversity of a community in terms of the whole ecosystem. The direction of the vector is determined by both abundance and combination of the species.

Mathematically, the simplest way to estimate the difference between two vectors is to calculate the angle between them. Based on this, it is possible to define the dissimilarity, as we demonstrate here.

If one denotes the values in the vector as 1 for represented species (species found at the community/site) and 0 for non-represented species in the aforementioned coordinate, then the two coordinates representing each site ($\mathbf{V}_1$ and $\mathbf{V}_2$) can be

https://doi.org/10.1017/pab.2024.40 Published online by Cambridge University Press

expressed as:

$$\mathbf{V}_1 = (\underbrace{1, 1, 1, 1, 1}_{s_{12}}, \underbrace{1, 1, 1, 1}_{N_1 - S_{12}}, \underbrace{0, 0, 0}_{N_2 - S_{12}}), \tag{2}$$

$$\mathbf{V}_2 = (\underbrace{1, 1, 1, 1, 1}_{S_{12}}, \underbrace{0, 0, 0, 0}_{N_1 - S_{12}}, \underbrace{1, 1, 1}_{N_2 - S_{12}}). \tag{3}$$

The order of the numbers in these coordinates does not influence the value calculated through the dot product. It is therefore recommended that each coordinate be divided into three sections for convenience of visualization, as in equations (2) and (3): shared species, species only present in the first community, and species only present in the second community.

Based on this, it is possible to calculate the angle between the two vectors (θ):

$$\theta = \langle \mathbf{V}_1, \mathbf{V}_2 \rangle = \cos^{-1} \frac{\mathbf{V}_1 \cdot \mathbf{V}_2}{|\mathbf{V}_1||\mathbf{V}_2|} = \cos^{-1} \left(\sum_{n=1}^{N_1+N_2-S_{12}} \frac{V_{1,n} V_{2,n}}{|\mathbf{V}_1||\mathbf{V}_2|} \right)$$
$$= \cos^{-1} \frac{S_{12}}{\sqrt{N_1 N_2}}, \tag{4}$$

where n is the nth component of the vectors, magnitude of $\mathbf{V}_1$, $|\mathbf{V}_1| = \sqrt{N_1 \cdot 1^2} = \sqrt{N_1}$, and $|\mathbf{V}_2| = \sqrt{N_2}$. As no components of the coordinate can be negative ($V_{1,n} \geq 0$, $V_{2,n} \geq 0$), naturally, $\frac{S_{12}}{\sqrt{N_1 N_2}} \in [0, 1]$, and especially for two identical communities ($S_{12} = N_1 = N_2$), $\frac{S_{12}}{\sqrt{N_1 N_2}} = 1$. This coefficient within the above inverse trigonometric function is termed the Otsuka coefficient (Peters 1968), and when it falls in the interval [0,1], the range of this inverse trigonometric function should be [0, π/2], that is, $\theta \in [0, \pi/2]$. To make this concept more readily understandable, the angle is further normalized by π/2, and we define this parameter as a new dissimilarity D:

$$D = \frac{2\theta}{\pi} = \frac{2}{\pi} \cos^{-1} \frac{S_{12}}{\sqrt{N_1 N_2}}. \tag{5}$$

Therefore, for two communities with adequate numbers of represented taxa (e.g., totaling at least on the order of 10), if there are no shared species between the communities, the two vectors are orthometric, and $D = 1$. In contrast, if all the species from the two sites are identical, then $S_{12} = N_1 = N_2$, and $D = 0$. In other words, dissimilarity becomes evident as the value of D approaches 1, whereas similarity manifests as it approaches 0. However, great care should be exercised if the two vectors are extremely sparse (i.e., if the total number of observations is very small, or many species are underrepresented), as their orthogonality ($D = 1$) might be a false indicator. This holds true for any kind of definition of dissimilarity. Nevertheless, in normal cases with a sufficient number of samples, D can genuinely reflect the variation in species diversity along an environmental or spatial gradient.

A Statistical Expression with Consideration of Species Abundance

In the above definition of dissimilarity, whether a species exists or not is only roughly defined by 1 or 0. For improved accuracy, we can define the values in a coordinate with the statistical parameter p_i, taking into account the abundance of each species. Under different scenarios, this statistical parameter can have different meanings (but comparisons must be made at the same scale). For example, p_i could be:

1. The number of times n_i (or frequencies $f_i = n_i/N$, where N is the total number of observations) that species i is represented in the case. Due to the normalization process involved in our calculation of dissimilarity (i.e., eqs. 4 and 5), the results calculated with n_i and f_i are the same (direction of the coordinate stays unchanged during normalization). In this way, the abundance of the species is considered.
2. The number of species belonging to genus i that exist at a certain site (n_i). Similarly, one could also use its frequency f_i to compute the dissimilarity, where $f_i = n_i/N_i$, with N_i being the total number of species that this genus has within a certain large-scale scenario (e.g., a continent or geological time period).

This statistical parameter can also be endued with a probability of existence within a hierarchical relation (i.e., the diversity of existing species within the same genus or the diversity of existing genera within the same family). Based on this, for two different sites, the coordinates can be written as:

$$\mathbf{V}_1 = (\underbrace{p_{1,1}, p_{1,2}, \ldots, p_{1,S_{12}-1}, p_{1,S_{12}}}_{S_{12}}, \underbrace{p_{1,S_{12}+1}, \ldots, p_{1,N_1}}_{N_1 - S_{12}}, \underbrace{0, 0, 0}_{N_2 - S_{12}}), \tag{6}$$

$$\mathbf{V}_2 = (\underbrace{p_{2,1}, p_{2,2}, \ldots, p_{2,S_{12}-1}, p_{2,S_{12}}}_{S_{12}}, \underbrace{0, 0, 0}_{N_1 - S_{12}}, \underbrace{p_{2,S_{12}+1}, \ldots, p_{2,N_2}}_{N_2 - S_{12}}). \tag{7}$$

where $p_{1,i}$ and $p_{2,i}$ are the parameters obtained with data from the first and second sites, respectively; and N_1 and N_2 are the total numbers of observations at each site. Hence, the dissimilarity can be defined as:

$$D = \frac{2\theta}{\pi} = \frac{2}{\pi} \cos^{-1} \frac{\mathbf{V}_1 \cdot \mathbf{V}_2}{|\mathbf{V}_1||\mathbf{V}_2|}$$
$$= \frac{2}{\pi} \cos^{-1} \frac{\sum_{i=1}^{S_{12}} p_{1,i} p_{2,i}}{\sqrt{\left(\sum_{j=1}^{N_1} p_{1,j}^2\right)\left(\sum_{k=1}^{N_2} p_{2,k}^2\right)}}, \tag{8}$$

where j and k are the jth and kth parameters of Site 1 and Site 2. If there is significant similarity between the two sites, D will be close to 0, and if the difference is strong, then D will approach 1.

Balance Index for Occurrences/Origination–Extinction

An advantage of using angles instead of cosine values to characterize dissimilarity is that they obey the associative law of addition. That is to say, angle A plus angle B equals angle $(A + B)$, whereas $\cos(A)$ plus $\cos(B)$ does not equal $\cos(A + B)$. This means we can split the angle (or a normalized angle) denoting dissimilarity into two parts to quantify the relative contribution of increases and decreases in the abundance of taxa.

Herein, a mean vector ($\mathbf{V}_m$) is employed to split the angle (θ) into two parts:

$$\mathbf{V}_m = \frac{\mathbf{V}_1 + \mathbf{V}_2}{2}. \tag{9}$$

https://doi.org/10.1017/pab.2024.40 Published online by Cambridge University Press

The angle between the mean vector and vector 1 ($\mathbf{V}_1$) is θ_1, and the angle between the mean vector and vector 2 ($\mathbf{V}_2$) is θ_2, defined as:

$$\theta_1 = \left\langle \mathbf{V}_1, \frac{\mathbf{V}_1 + \mathbf{V}_2}{2} \right\rangle = \cos^{-1}\left(\frac{|\mathbf{V}_1|}{2|\mathbf{V}_2|} + \frac{\mathbf{V}_1 \cdot \mathbf{V}_2}{2|\mathbf{V}_1||\mathbf{V}_2|}\right), \quad (10)$$

$$\theta_2 = \left\langle \mathbf{V}_2, \frac{\mathbf{V}_1 + \mathbf{V}_2}{2} \right\rangle = \cos^{-1}\left(\frac{|\mathbf{V}_2|}{2|\mathbf{V}_1|} + \frac{\mathbf{V}_1 \cdot \mathbf{V}_2}{2|\mathbf{V}_1||\mathbf{V}_2|}\right), \quad (11)$$

and therefore,

$$\theta = \theta_1 + \theta_2. \quad (12)$$

As shown in Figure 1A, only when the increase is identical to the decrease can triangle *Oca* and triangle *Ocb* be said to be congruent, with θ_1 equal to θ_2 and the mean vector being the angular bisector of θ (angle *bOa*). If the increasing rate is much higher (i.e., larger vector magnitude with larger angle *aOx*), the mean vector becomes closer to vector 2, with a larger θ_1 (Fig. 1B).

The law of addition holds true if the angles are normalized with $\pi/2$:

$$D_1 = \frac{2\theta_1}{\pi}, D_2 = \frac{2\theta_2}{\pi}, \text{ and } D = D_1 + D_2, \quad (13)$$

where D_1 and D_2 are partial dissimilarities. Because D_1 increases with the number of occurrences, we can define a balance index for occurrences (γ):

$$\gamma = \frac{D_1}{D} = 1 - \frac{D_2}{D}. \quad (14)$$

When the increase in the number of occurrences is equal to the decrease, $D_1 = D_2$ and $\gamma = \frac{D_1}{2D_1} = 0.5$, and the taxonomic flux is balanced. When the rate of increase is higher, $D_1 \in (0.5, 1]$, and when the rate of decrease is higher, $D_1 \in [0, 0.5)$. When using 1/0-based descriptions (i.e., 1 for presence and 0 for absence, as in eqs. 2 and 3), the obtained result will inform on the balance between the origination and extinction components of dissimilarity (the balance index for origination and extinction), similar to that in Bush et al. (2019). However, it should be noted that this balance index only works when $\mathbf{V}_1 \neq \mathbf{V}_2$. If the two vectors are equal, that is, they are overlapped, we therefore by default consider $\gamma = 0.5$.

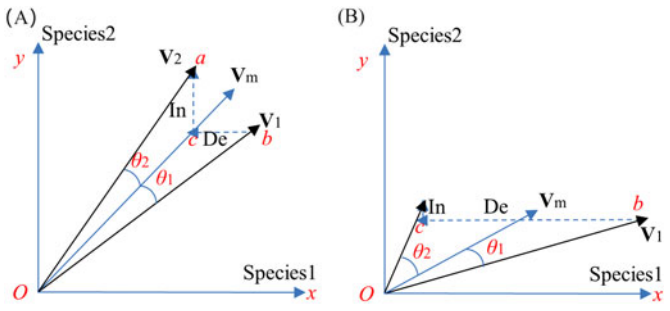


Figure 1. Diagram showing how the angle representing the dissimilarity between two vectors can be divided into increased (In) and decreased (De) components of occurrences. Only when the gained and lost occurrences are balanced **(A)**, can the two angles split by the mean vector be equal. If the loss of occurrences is higher **(B)**, the mean vector becomes closer to vector 1.

Simple Demonstration and Convergence Study

In this section, we present a simple case study illustrating the difference between the absolute species turnover in equation (1) and the metric proposed herein. Table 1 shows observations from four different sites:

If one calculates beta diversities for site 1 versus site 2 and site 3 versus site 4 using equation (1), the same value of 3 is obtained. However, the community from site 1 only shows small differences from that at site 2, while the community from site 3 is very different from the one at site 4, with only one shared species.

In contrast, using the measure proposed herein, we can compute the dissimilarity (beta diversity here as well) between site 2 versus site 1 as $\beta_{2-1} = \frac{2}{\pi}\cos^{-1}\frac{11\cdot1+3\cdot0}{\sqrt{12\cdot13}} = 0.314$, and that between site 4 and site 3 as $\beta_{4-3} = \frac{2}{\pi}\cos^{-1}\frac{1\cdot1+13\cdot0}{\sqrt{2\cdot3}} = 0.732$, indicating that the communities from site 2 and site 1 are similar, while the communities from site 4 and site 3 are dissimilar. This provides a better explanation of the data presented in Table 1.

Our measure of dissimilarity shows little bias compared with the Morisita-Horn (M-H) dissimilarity (Horn 1966): $D_{\text{mh}} = 1 - \frac{2\sum V_{1,i}V_{2,i}}{\left(\frac{\sum V_{1,i}^2}{N_1^2} + \frac{\sum V_{2,i}^2}{N_2^2}\right)N_1N_2}$. For example, the following benchmark case has 10,000 random integers ranging from 1 to 20, and we have 21 testing cases (for comparison) where the *M*th case has *M* integers ranging from 1 to *M*($M \leq 20$; the 0th case has all-zero components; and the 20th case shall be equivalent to the benchmark, with its integers ranging from 1 to 20). As such, the proposed dissimilarity of the benchmark case versus the 10th cases (which share 10 elements with the benchmark case, as shown in Table 2) should analytically be $D = \frac{2}{\pi}\cos^{-1}\frac{500\cdot1000\cdot10+500\cdot0\cdot10}{500\sqrt{20}\cdot1000\sqrt{10}} = 0.5$, which is exactly "half the same," as it should be. On the other hand, the M-H dissimilarity should analytically be $D_{\text{mh}} = 1 - \frac{2\cdot(500\cdot1000\cdot10)}{\left(\frac{20\cdot500^2}{10,000^2} + \frac{10\cdot1000^2}{10,000^2}\right)10,000^2} = \frac{1}{3}$, which demonstrates severe computational bias. This computational bias is shown in Figure 2, where the proposed measure of dissimilarity is an antisymmetrical odd function about (10, 0.5) with better linearity between the metrics and number of non-shared observations, whereas the M-H dissimilarity is a convex function that exhibits no symmetry over "half-similarity." In other words, one shared sample among 20 (~0.856) is complementary to 19 shared samples among 20 (~0.144), and these two values add up to 1 in the proposed metrics.

In addition to computationally bias-free accuracy, convergence and robustness are also important features for evaluating our newly proposed measure of dissimilarity. To assess this, we created two datasets containing 2000 integral numbers. The first dataset has 10 different numbers (1 to 10), while the second dataset has 20 different numbers (1 to 20). These numbers are evenly and randomly distributed in the datasets. Dissimilarities between the two datasets were then calculated with certain numbers of observations extracted from the datasets (from 50 to 2000, at intervals of 50). Seven data series were generated in this way. The estimated beta diversities versus the number of observations used in the calculations are shown in Figure 3.

As shown in Figure 3, as the number of observations increases, the obtained dissimilarity between the two datasets converges on

https://doi.org/10.1017/pab.2024.40 Published online by Cambridge University Press

Table 1. Samples from four sites, where A–N represent different species.

	A	B	C	D	E	F	G	H	I	J	K	L	M	N
Site 1	X	X	X	X	X	X	X	X	X	X	X	X		
Site 2	X	X	X	X	X	X	X	X	X	X	X		X	X
Site 3	X											X		
Site 4	X												X	X

the analytical result of 0.5. The mean absolute error is 5% for 100 observations, which is 5 times the number of features (20). The mean absolute error decreases to 2.5% at around 260 observations, which is 13 times the number of features. This indicates that the proposed measure of dissimilarity will perform well (2.5% error) as long as the total number of the observations in the dataset exceeds around 13 times the number of data features (e.g., taxa).

From the these analyses, it is evident that our proposed measure of vector-based dissimilarity functions well at different observation sizes and abundances and can accurately determine the dissimilarity between two datasets. It is not biased by the number of overlapping features and readily converges on the analytical result.

To evaluate the balance index for occurrences, we set up a test case with the following vectors. Partial dissimilarities and balance indices were computed with comparisons between $\mathbf{V}_2 \sim \mathbf{V}_7$ and $\mathbf{V}_1$:

$$
\begin{aligned}
&\mathbf{V}_1 = [1, 1, 1, 1, 1, 0, 0, 0, 0, 0],\\
&\mathbf{V}_2 = [1, 1, 1, 1, 0, 1, 0, 0, 0, 0], \quad D_{1_2\text{-}1} = D_{2_2\text{-}1} = 0.2048, \quad \gamma_{2\text{-}1} = 0.5;\\
&\mathbf{V}_3 = [1, 1, 1, 0, 0, 1, 1, 0, 0, 0], \quad D_{1_3\text{-}1} = D_{3_2\text{-}1} = 0.2952, \quad \gamma_{3\text{-}1} = 0.5;\\
&\mathbf{V}_4 = [1, 1, 1, 1, 0, 1, 1, 1, 0, 0], \quad D_{1_4\text{-}1} = 0.2871, \quad D_{2_4\text{-}1} = 0.2402, \quad \gamma_{4\text{-}1} = 0.5445;\\
&\mathbf{V}_5 = [1, 1, 0, 0, 0, 1, 0, 0, 0, 0], \quad D_{1_5\text{-}1} = 0.2871, \quad D_{2_5\text{-}1} = 0.3729, \quad \gamma_{5\text{-}1} = 0.4304;\\
&\mathbf{V}_6 = [1, 1, 1, 1, 2, 0, 0, 0, 0, 0], \quad D_{1_6\text{-}1} = 0.1145, \quad D_{2_6\text{-}1} = 0.0903, \quad \gamma_{6\text{-}1} = 0.559;\\
&\mathbf{V}_7 = [1, 1, 1, 1, 0, 30, 0, 0, 0, 0] \quad D_{1_7\text{-}1} = 0.8434, \quad D_{2_7\text{-}1} = 0.1187, \quad \gamma_{7\text{-}1} = 0.877;
\end{aligned}
$$

This shows that, if the increase of taxa is equal to the decrease compared with $\mathbf{V}_1$ (i.e., $\mathbf{V}_2$ and $\mathbf{V}_3$), the balance index is 0.5, and the magnitudes of partial dissimilarities increase with the magnitude of taxonomic flux. However, if the magnitude of increase is higher than the magnitude of the decreases ones (i.e., $\mathbf{V}_4$, one extinction, three originations), the balance is broken, and the index exceeds 0.5, and vice versa for $\mathbf{V}_s$. An increase in species abundance (i.e., $\mathbf{V}_6$ and $\mathbf{V}_7$) also leads to an increase in the balance index.

Materials

Under present ichnological practice, diagnostics of trace fossils experience unavoidable uncertainties caused by behavioral diversity, taphonomic effects, and observer biases, leading to synonyms and problematica. Therefore, the authors employed a well-tuned but conservative dataset containing widely accepted trace fossil taxa from the Ediacaran and Cambrian periods, mainly from Mángano and Buatois (2016), with putative body fossils like *Nenoxites* (*Shaanxilithes*) (Zhu et al. 2017; Luo and Miao 2020; Mángano and Buatois 2020) removed, and supplemented with new data from other relevant studies. This included *Cochlichnus* (Webby 1970; Darroch et al. 2021) from shallow-marine (i.e., wave-influenced region in this paper) deposits of the latest Ediacaran Torrowangee Group of western New South Wales and the Nama Group of southern Namibia, as well as *Diplichnites* from the Shibantan Member of the upper Dengying Formation in the Yangtse Gorges area in South China (Chen et al. 2018), which may represent the earliest trackways made by bilaterian animals with paired appendages. Additionally, *Radulichnus* (Seilacher and Hagadorn 2010) and *Lockeia* (Crimes and Fedonkin 1994; Pandey et al. 2014; Kaur et al. 2021) from Ediacaran and Cambrian shallow-marine deposits, *Bergaueria* (Alpert 1973) and *Torrowangea* (Zhuravlev and Riding 2000) from Ediacaran and Cambrian shallow- and deep-marine deposits, *Thalassinoides* (Zhang et al. 2017), *Gordia* (Buatois et al. 2014), *Parapsammichnites* and *Streptichnus* from Ediacaran shallow seas (Buatois et al. 2018; Darroch et al. 2021), *Archaeonassa* (Hofmann et al. 2012), *Didymaulichnus* (Jensen and Mens 2001) and *Trypanites* (James et al. 1977) from Cambrian shallow-marine deposits, *Saerichnites* from Cambrian deep-marine deposits (Buatois and Mángano 2004), and *Protopaleodictyon* (Zhuravlev and Riding 2000) from Cambrian shallow- and deep-marine deposits were added to the dataset. *Treptichnids* from the Nama Group is tentatively combined into *Treptichnus* due to possible variations from behaviors or taphonomy. The occurrences are recorded at the "member" scale, unless the formation has not been subdivided into members. The full dataset is shown in Table 3.

There may be uncertainties related to the age, behavioral categorization, and taxonomic identifications of some of the trace fossils in our dataset, as well as possible sampling biases to contend with. However, bounded by the central limit theorem

https://doi.org/10.1017/pab.2024.40 Published online by Cambridge University Press

Table 2. Theoretical probability of occurrence of each element in the benchmark and the 10th testing case.

	1	2	3	…	9	10	11	12	…	18	19	20
Benchmark	500	500	500	500	500	500	500	500	500	500	500	500
10th case	1000	1000	1000	1000	1000	1000	0	0	0	0	0	0

(Kwak and Kim 2017), the distribution of these data approximates a Gaussian distribution around the "true value." Consequently, background noise will be minimized so long as the number of observations is sufficiently large and the computational algorithm is converged, as demonstrated in the previous section.

Results and Discussion

Ediacaran–Cambrian Trace Fossil Dissimilarity, Origination, and Extinction

The Ediacaran preserves the oldest evidence of large and morphologically complex multicellular organisms, including some of Earth's earliest animals, documenting the first appearance of convincing bilaterian traces (Gehling et al. 2014; Mángano and Buatois 2016; Chen et al. 2019; Evans et al. 2022). As the sensory and locomotory capabilities of early metazoans evolved, they started to have a bigger impact on their environment by disturbing the substrate and creating vertical burrows (Cribb et al. 2019), enhancing the exchange of nutrients between the pelagic and benthic realms (Erwin and Tweedt 2012; Buatois et al. 2018). When the substrate became increasingly bioturbated and heterogeneous during the early part of the Cambrian (i.e., the AR), it posed challenges to organisms grazing on microbial mats (which had served to stabilize substrates during much of the Proterozoic), which is thought to have driven changes in animal morphology, function, and behavior. This evolutionary divergence in response to changes in the nature of the substrate is referred to as the Cambrian substrate revolution (Bottjer et al. 2000). To help decipher the evolution of early metazoans during this interval, we analyzed the dissimilarity and balance index of trace fossils from the Ediacaran–Cambrian.

Using the data in Table 3, we obtained six vectors for the corresponding six time periods. For example, after removing columns with all-zero elements, the vectors for the White Sea and Nama Group are (3, 1, 0, 0, 0, 2, 3, 9, 6, 1, 0, 0, 8, 3, 0, 1, 0) and (1, 1, 2, 1, 2, 0, 5, 14, 4, 0, 1, 1, 10, 0, 1, 7, 4), respectively. We used these to calculate dissimilarity and the balance index for occurrences for each pair of time bins and plotted these against time, with the results shown in Figure 4. Based on this, we found that dissimilarity (Fig. 4A) and both balance indices (Fig. 4B,C) peaked across the interval between the Ediacaran Nama Group and the Cambrian Fortunian Stage, associated with a dramatic increase in global diversity and abundance of trace fossils (Mángano and Buatois 2016). These include simple horizontal traces like *Gordia*, *Helminthopsis*, and *Helminthoidichnites*, thought to be made by vermiform primary consumers (mat grazers) that lived on Ediacaran-style microbial substrates. Such traces tend to have limited curvature with simple geometries, and no specific ethological taxis can be identified from them. These simple traces persisted into the Cambrian (Buatois et al. 2014). However, by the Fortunian, more morphologically complex traces started to appear, like *Cruziana* and *Rusophycus*, which are thought to have been produced by arthropods; pentaradially symmetrical *Asteriacites* (a putative asterozoan resting trace; Knaust and Neumann 2016); *Teichichnus* (a passively filled subvertical spreite burrow thought to be created by arthropods or annelid worms; Knaust 2018); and *Dactyloidites* (thought to be made by polychaetes or worms with a suspension-feeding life mode; Curran and Glumac 2022). Evidence of sharp turnings, self-crossing or avoidance of self-crossing, displacement of sediment, and taxis can be observed in several of these traces. This increase in the abundance and complexity of traces across the Ediacaran/Cambrian boundary also informs on the evolution of the tracemakers, implying the emergence of ecosystem engineers, secondary consumers, detritivores, and scavengers with morphologically varied body plans and feeding strategies. Based on study of the trace fossil record, major new animal body

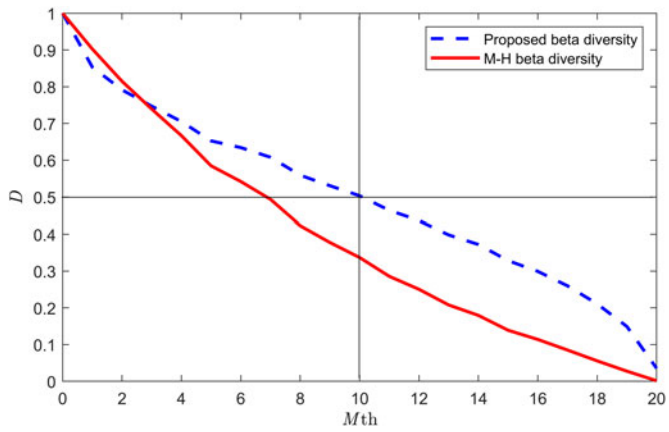


Figure 2. Variation in dissimilarity (*D*) across a number of shared elements (*M*th case) compared with the benchmark: proposed vector-based dissimilarity versus Morisita-Horn (M-H) dissimilarity.

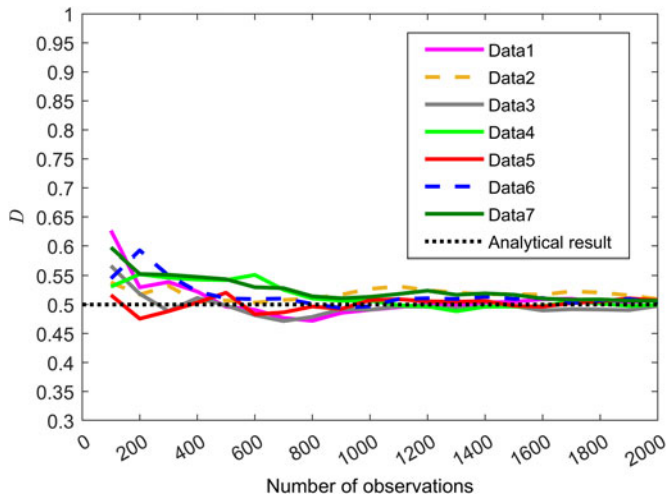


Figure 3. Convergence study. The obtained dissimilarity (*D*) converges on 0.5 with increasing numbers of observations.

https://doi.org/10.1017/pab.2024.40 Published online by Cambridge University Press

Table 3. Marine trace fossils from the Ediacaran to Cambrian Epoch 2. Numbers in cells indicate the number of sites where a given ichnogenus has been found. Different cell shadings correspond to shallow (gray), deep (orange), and eurybathic (blue) trace fossils. W, White Sea; N, Nama; F, Fortunian; S2, Cambrian Stage 2; S3, Cambrian Stage 3; and S4, Cambrian Stage 4. Ethological categories (behaviors): A, agrichnia (farming or parenting); C, cubichnia (resting); D, domichnia (dwelling); E, equilibrichnia (balancing its position against sedimentary events); F, fodichnia (feeding); P, pascichnia (grazing); and R, repichnia (locomotion). Functional groups: B, biodiffusive bioturbators; C, conveyors; E, epifaunal bioturbators; G, gallery biodiffusors; R, regenerators; and S, surficial modifiers.

	W	N	F	S2	S3	S4	Behavior	Functional group
Alcyonidiopsis				1			F	S
Allocotichnus			1				R	E
Altichnus				1	1		D	B
Archaeonassa	3	1	2	3	3	4	P	E
Arenicolites			1	8	15	9	D	R
Asaphoidichnus			1		1		R	E
Asteriacites			1	1		1	C	E
Asterosoma					2	1	D,F	S,C
Astropolichnus				2	7	1	D	B
Bergaueria	1	1	2	4	14	9	D	S
Bifungites					1	1	D	R
Cheiichnus				1	4	1	C	B
Circulichnis			1				F	S
Cochlichnus		2	7	2	7	3	R	E
Conichnus		1	1	1			D,C	S
Conostichus					2		D	B
Cruziana			3	10	21	23	R	E
Curvolithus			6	4	4	1	R	E
Cylindrichnus				1	2		D	C
Dactyloidites			1		7	3	F	B
Dendrorhaph			1				A	S
Didymaulichnus			8	6	3	2	P	E,S
Dimorphichnus			2	1	13	11	P	E
Diplichnites		1	5	4	12	8	R	E
Diplocraterion				8	13	8	D,E	C
Diplopodichnus			1				R	E
Dolopichnus				1			D	B
Elingua					1	1	C	S
Fustiglyphus					1	1	R	S
Epibaion	2						C	E
Gordia	3	5	4	4	4	3	P	E,S
Gyrolithes			9	7	8	2	D	R
Halopoa					3	2	F	C
Helminthoidichnites	9	14	6	6	9	4	P	E
Helminthopsis	6	4	8	5	10	4	P	E
Kimberichnus	1						P	E

(*Continued*)

plans and feeding modes seem to have appeared across the boundary between the Ediacaran and Cambrian periods, and this event has been termed the Fortunian diversification event (FDE) (Mángano and Buatois 2016). This is thought to be an expression of the Cambrian information revolution (CIR) (Plotnick et al. 2010; Hsieh et al. 2022), which was characterized by the development of more advanced sensory, cognitive, and locomotory capabilities. As ecological niches were progressively filled during this evolutionary radiation, the diversification of traces slowed, with the magnitude of dissimilarity steadily decreasing through the Cambrian (Fig. 4A). Ichnodissimilarity dropped to a low point of 0.161 across the boundary between the third and fourth stages of the Cambrian, indicating an evident similarity in ichnotaxa from these two stages.

The general profile of ichnodissimilarity over the Ediacaran–Cambrian (Fig. 4A) closely matches estimates of diversification rates for marine animals based on sampling-standardized analyses (Na and Kiessling 2015), which show a peak in the Fortunian, followed by a decline through the Cambrian. However, comparing ichnodissimilarity to the global and beta diversities of marine animals, which peaked at around Cambrian Stage 3 (Sepkoski 1998; Na and Kiessling 2015; Fan et al. 2020), reveals a stronger asynchrony between the trace and body fossil records. This asynchrony suggests that the overall dissimilarity of trace fossils more closely corresponds to the diversification of major animal body plans and behaviors at higher taxonomic levels (Zhang and Shu 2021) than it does to genus- or species-level diversity.

https://doi.org/10.1017/pab.2024.40 Published online by Cambridge University Press

Table 3. (*Continued.*)

Lingulichnus				1			D	R
Lockeia		1		1	1	2	C	S
Megagrapton					1	2	A	G
Monocraterion					2	1	D	B
Monomorphichnus			6	15	15	14	E,F	E
Multilamella						1	F	S
Multilaqueichnus					1		F	S
Multina			1	1	1	1	F	G
Nereites			1		2	1	P	B
Oldhamia			12	8	14	11	F,P	S
Parapsammichnites		1					C	E
Palaeophycus	8	10	16	16	30	20	D	G
Paleodictyon				1	4	3	A	G
Petalichnus				1	1	1	R	E
Phycodes			4	7	14	7	F	S
Pilichnus			1				F	S
Planolites			16	21	30	18	F	S
Protichnites						1	R	E
Protopalodictyon			1	1			A	G
Protovirgularia				1	2	2	R	B
Psammichnites			9	16	21	12	F,P	B
Radulichnus	3		1	1			P	E
Rhizocorallium			1	3	9	3	D,F	C
Rosselia				2	7	5	D,F	C
Rusophycus			10	19	31	23	C	E
Saerichnites			5	5	7	4	A,F	E
Skolithos				15	40	30	D	R
Streptichnus		1					F	S
Syringomorph				1	5	4	D	C
Taenidium					1		F	C
Tasmanadia			2				R	E
Teichichnus			4	11	19	8	D,F	C
Thalassinoides			1		1	2	D,F	G
Torrowangea	1	7	2		4		P	E
Treptichnus		4	31	14	13	7	F	B,C
Trichophycus					4	3	D,F	G
Trypanites						1	D	R
Volkichnium			1				F	S
Zoophycos					2	2	F	C

Unlike ichnodissimilarity, the balance index for occurrences shows a second peak at the start of Cambrian Stage 3 (Fig. 4B). The balance index for origination and extinction is only slightly above 0.5, demonstrating that this peak indicates an increase in the abundance of existing ichnotaxa, rather than the origination of new trace fossils. This could be associated with the diversification and expansion of existing animals in a stable ecological system, as well as the divergence of crown-group animals with similar body plans and ethological tendencies (Na and Kiessling 2015), consistent with suggestions of a two-phase model for the evolution of stem-group animals and expansion and divergence of crown-group animals during the Cambrian (Zhuravlev and Wood 2018; Zhang and Shu 2021).

Across the boundary between Cambrian Stages 3 and 4, the decrease in the occurrences of trace fossils exceeded the increased occurrences for the first time, resulting in balance indices less than 0.5 (Fig. 4B). A decline in marine bioturbation at this time was also noted by Buatois and Mángano (2016). This could reflect a reduction in the abundance and diversity of marine animals during this interval, corresponding to regional disappearance/extinction of some groups (Na and Kiessling 2015). This may be related to the Sinsk event, an episode of widespread shallow-marine anoxia (Na and Kiessling 2015; Zhuravlev and Wood 2018).

Behavioral Activities

Our analyses of ichnodissimilarity also shed light on the evolution of animal behaviors during the Ediacaran–Cambrian. For those trace fossils that have been interpreted as the result of two different behaviors, such as the funnel-shaped vertical concentric burrow *Rosselia*, which could be the product of both dwelling and

https://doi.org/10.1017/pab.2024.40 Published online by Cambridge University Press

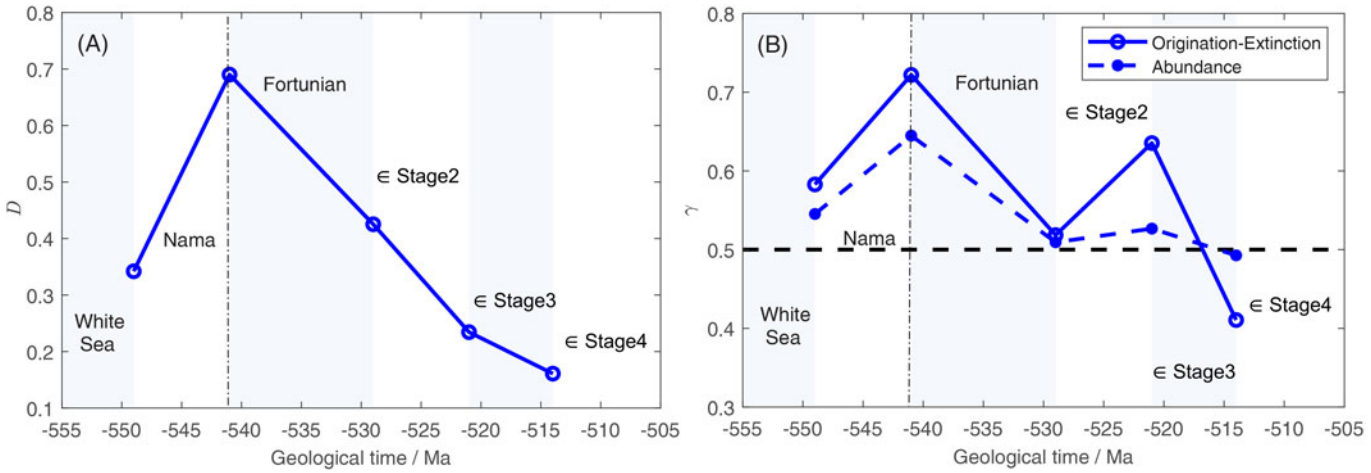


Figure 4. Ichnological dissimilarity **(A)** and balance indices **(B)** across the Ediacaran–Cambrian. **A,** Dissimilarity is most evident at the Ediacaran/Cambrian boundary, decreasing through the Cambrian. **B,** Balance indices for occurrences (line) and origination and extinction (dashed line) across the Ediacaran–Cambrian. Values above 0.5 indicate that the contribution from increasing numbers of taxa is greatest; values below 0.5 indicate that the contribution from the loss of taxa or abundance is greatest. The balance index for occurrences peaks at the boundaries between the Ediacaran and the Cambrian and between Cambrian Stages 2 and 3, before declining at the boundary between Cambrian Stages 3 and 4. The second peak is a result of increased occurrences rather than the origination of new body plans, as shown by the low value of the balance index for origination and extinction.

feeding behaviors, the number of occurrences in each time interval was halved in the corresponding ichnological matrix; for example, the occurrence of *Rosselia* as a domichnia or repichnia during the Ediacaran and Cambrian periods is denoted as (0, 0, 0, 1, 3.5, 2.5). In this way, the matrix for each behavioral (ethological) category was estimated. For example, cubichnia gives the following matrix:

$$\begin{array}{c} \\ \textit{Asteriacites} \\ \textit{Cheiichnus} \\ \textit{Conichnus} \\ \textit{Elingua} \\ \textit{Epibaion} \\ \textit{Lockeia} \\ \textit{Parapsammichnites} \\ \textit{Rusophycus} \end{array} \begin{array}{c} \begin{array}{cccccc} W & N & F & S2 & S3 & S4 \end{array} \\ \begin{bmatrix} 0 & 0 & 1 & 1 & 0 & 1 \\ 0 & 0 & 0 & 1 & 4 & 1 \\ 0 & 0.5 & 0.5 & 0.5 & 0 & 0 \\ 0 & 0 & 0 & 0 & 1 & 1 \\ 2 & 0 & 0 & 0 & 0 & 0 \\ 0 & 1 & 0 & 1 & 1 & 2 \\ 0 & 1 & 0 & 0 & 0 & 0 \\ 0 & 0 & 10 & 19 & 31 & 23 \end{bmatrix} \end{array} \quad (16)$$

where the eight rows correspond to ichnogenera representing different resting behaviors and the six columns denote the six time periods. *Parapsammichnites* is interpreted as a resting/struggling trace of segmented worms in response to environmental stress for its abundant but short and frequent loops on the same surface. The dissimilarity between two intervals was calculated using the corresponding columns of vectors.

We selected four ethological categories (agrichnia, domichnia, pascichnia, and repichnia) and reconstructed matrices for each of these based on the data in Table 3. The ichnodissimilarity and balance indices calculated for each behavior across this interval are shown in Figure 5.

The global ichnodiversity and frequencies of occurrence of grazing traces (pascichnia) increased during the Fortunian Stage (Table 3), resulting in a peak in dissimilarity of 0.615 at the Ediacaran/Cambrian boundary (Fig. 5A). This evident change was a result of origination, as evidenced by the peak of the balance index for origination and extinction (Fig. 5C). Grazing traces increased in size during the Cambrian and began to exhibit more complex behaviors (Mitchell et al. 2022) like space-filling patterns reflecting phobotaxis (i.e., avoiding crossovers of previous trails), thigmotaxis (i.e., staying close to the original trails), and strophotaxis (i.e., periodic 180° turns), as evidenced by trace fossils such as *Psammichnites* and *Oldhamia* (Seilacher et al. 2005; Mángano and Buatois 2016; Gougeon et al. 2018a) (Fig. 6A,B). This indicates that Cambrian grazers (e.g., mollusks; Wang and Rahman 2023) were better at exploring the substrate than Ediacaran forms and strongly implies changes to their cognitive, sensory, and navigational capabilities (Hsieh et al. 2022). This evolutionary event is referred to as the CIR (Plotnick et al. 2010). With the enhanced capacities for motility that animals evolved following the Fortunian, the microbial matground became more and more patchy, and as a result, the diversification rate of grazing behaviors slowed down after the Fortunian. In contrast, the balance index for occurrences at this interval is very close to 0.5 (Fig. 5B), meaning the occurrence of new grazing behaviors and body plans was balanced by a reduction in abundance of existing ones, possibly due to the crowded niche at the water–substrate interface.

For dwelling traces (domichnia), peak dissimilarity (0.487) was reached at the boundary between the Fortunian and Cambrian Stage 2 (Fig. 5A), associated with increases in their frequency of occurrences (Fig. 5B), as well as behavioral/body plan innovations (Fig. 5C) that rooted from Fortunian and prospered during Cambrian Stage 2. This process was characterized by the appearance and abundance of vertical burrows like *Skolithos*, *Arenicolites*, *Gyrolithes*, and *Rosselia*, as well as U-shaped burrows with spreites, like *Diplocraterion* (Fig. 6C–E). Oblique to subvertical burrows with actively filled spreites (Knaust 2013), like *Teichichnus* and *Rhizocorallium*, were also abundant during this interval. These vertical or subvertical burrows may indicate the evolution of new and more active feeding strategies (Zamora et al. 2017), biomineralized hard parts (to remove or displace sediments; Roy and Purohit 2018), and/or possible predation pressure (Wilson et al. 2012). The diversification of these dwelling traces, thought to be created by crustaceans and other suspension-feeding animals (Buatois et al. 2020), coincided with a shift in

https://doi.org/10.1017/pab.2024.40 Published online by Cambridge University Press

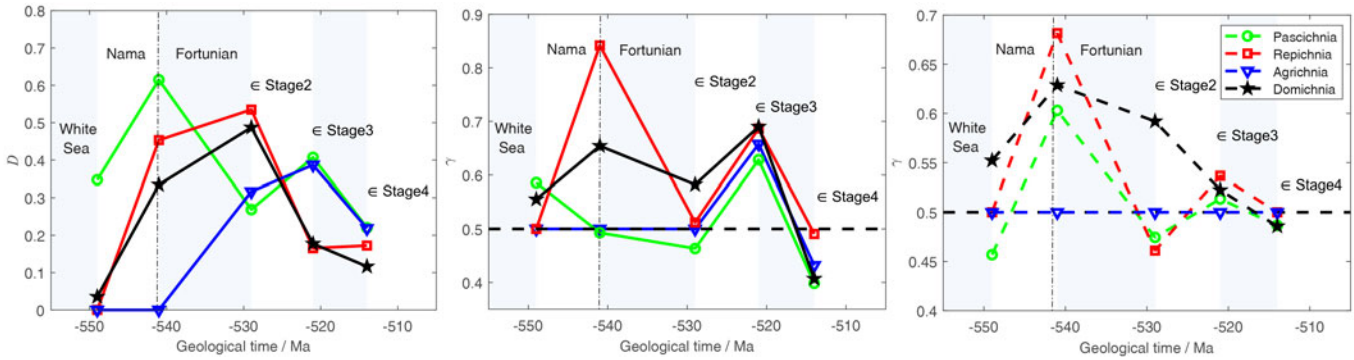


Figure 5. Evolution of animal behaviors across the Ediacaran–Cambrian. **A,** Dissimilarity. Grazing traces (pascichnia) peak at the Ediacaran–Cambrian interface, while dwelling traces (domichnia) and locomotion traces (repichnia) peak later on, after the Fortunian Stage. Complicated behaviors like parenting and farming (agrichnia) experienced a later divergence at the end of Cambrian Stage 2. In all cases, dissimilarity decreased after Cambrian Stage 3. **B,** Balance index for occurrences. Pascichnia and agrichnia reached the peak of diversity and abundance at the interface between Cambrian Stages 2 and 3, while repichnia and domichnia had another peak at the Ediacaran–Cambrian interface. All the behaviors experienced reductions in abundance or even taxa at Cambrian Stage 4. **C,** Balance index for origination and extinction. All the categories but agrichnia peaked at the Ediacaran/Cambrian boundary, with repichnia and pascichnia experiencing a second smaller peak at the boundary between Cambrian Stages 2 and 3.

organism–substrate interactions (i.e., the displacement of sediment particles) from a diffusion-dominated stage to an advection-dominated stage (Tarhan 2018), which enhanced the exchange of nutrient particles between the water column and benthic and infaunal communities. After the Fortunian, the origination rate of new domichnia dropped, evidenced by reductions in the balance index for origination and extinction (Fig. 5C), perhaps reflecting the occupation of the associated living strategies and niches. Nevertheless, an increase in the frequency of occurrences (Fig. 5B) can be seen at the boundary between Cambrian Stages 2 and 3, potentially suggesting the presence of increasingly habitable environments, especially in high-energy shallow waters.

Locomotory traces (repichnia) show trends similar to those of domichnia, with a major peak in dissimilarity at the boundary between the Fortunian and Cambrian Stage 2 (Fig. 5A). This reflects the appearance of complex new body plans and behaviors, such as *Cruziana*, *Diplichnites* (Fig. 6F), and *Curvolithus* during the Fortunian diversification, evidenced by a peak in the balance index for origination and extinction at the Ediacaran/Cambrian boundary (Fig. 5C). This evolutionary radiation continued into Cambrian Stage 2, albeit at a relatively slower rate (shown by the lower magnitudes in both the balance indices), at which time existing locomotory traces like *Diplichnites* became more abundant, and new complex trackways like *Petalichnus*, *Protovirgularia*, and *Tasmanadia* first appeared (Mángano and Buatois 2016). These trackways from the Fortunian and Cambrian Stage 2 provide evidence for more enhanced mobility (e.g., stronger muscles attached to exoskeletons with joints) and maneuverability of primary and secondary consumers, producing stronger and deeper impressions in the substrate and more laterally extensive sediment displacement than grazing traces. Together with the aforementioned increase in vertical dwelling burrows, this contributed to the transformation of the substrate from a primarily two-dimensional matground to a three-dimensional mixground inhabited by diverse benthic animals during Cambrian Stage 2. Due to the heterogeneous nature of this mixground, feeding strategies shifted from slowly grazing the surface of the matground (i.e., pascichnia) to searching for food across long distances (i.e., repichnia). This transition marks the onset of the AR (Ichaso et al. 2022), with repichnia increasing in abundance during Cambrian Stage 3 (as illustrated by the high balance index for occurrences, alongside a low balance index for origination and extinction; Fig. 5B,C).

With the development of enhanced sensory, mobility, and maneuverability capabilities, benthic animals started to explore new feeding strategies, like farming of bacteria within a designed substrate topology, or new parenting strategies. This is termed agrichnia, and typical ichnotaxa include *Saerichnites* and *Paleodictyon* (Fig. 6G), and *Protopaleodictyon* (Morgan et al. 2019). Though some of these behaviors can be traced to earlier stages in the Cambrian, the biggest increase in the abundance of such trace fossils occurred during Cambrian Stage 3, giving the greatest dissimilarity and balance index for occurrences (Fig. 5A,B) at the boundary between Cambrian Stages 2 and 3. The taxonomic turnovers during this period were, however, basically balanced (Fig. 5C).

After Cambrian Stage 3, the dissimilarity of grazing, dwelling, locomotion, and farming traces all decreased (Fig. 5A), with all balance index for occurrences values lower than 0.5 (Fig. 5B), and domichnia and pascichnia even experienced a higher extinction rate (Fig. 5C). This indicates the decrease in frequency of occurrences and even loss of taxa during Cambrian Stage 4. This could be interpreted as an outcome of animals experiencing an overcrowded niche conditions, but might also be related to the decrease in global genus-level diversity of marine animals at this time due to anoxic events (Na and Kiessling 2015).

The balance indices for occurrences for domichnia and repichnia and the balance indices for origination and extinction for pascichnia and repichnia all show two distinct peaks (Fig. 5B,C), which parallel the patterns in the overall balance indices of Ediacaran–Cambrian trace fossils (Fig. 4B). This informs on the two-phase evolutionary pattern during this critical interval: a major evolutionary radiation occurred during the FDE, with the appearance of novel body plans and behaviors, as well as high frequency of occurrences among different localities. There is also a smaller second peak in the balance indices at the boundary between Cambrian Stages 2 and 3 (Fig. 4B), which was the result of an increase in occurrences, rather than origination (albeit origination was still higher than extinction). But agrichnia had not

https://doi.org/10.1017/pab.2024.40 Published online by Cambridge University Press

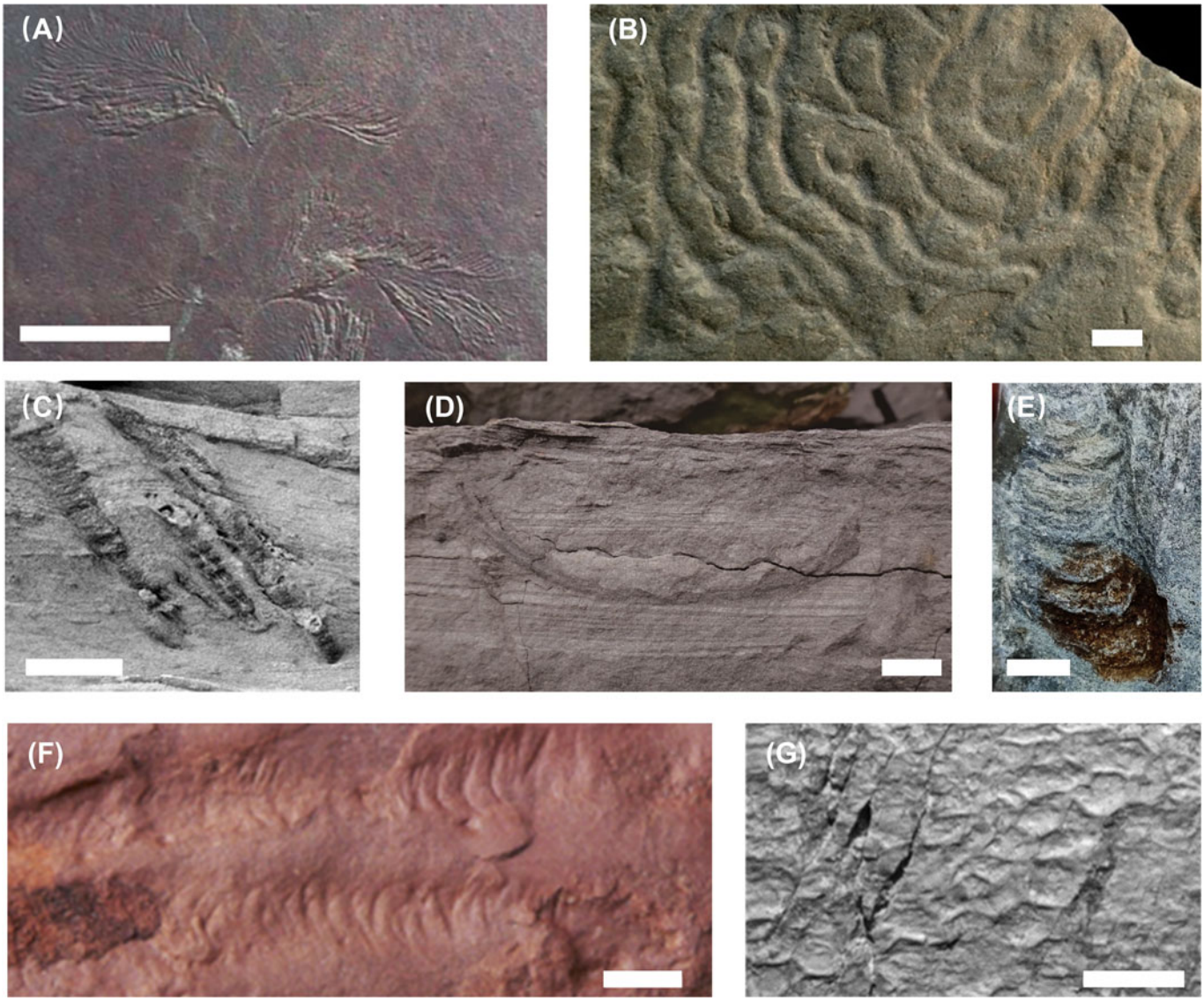


Figure 6. Typical Cambrian grazing trace fossils: *Oldhamia* **(A)** shows evidence of phobotaxis and thigmotaxis; *Psammichnites* **(B)** shows evidence of strophotaxis. These complex grazing traces first appeared in the Fortunian stage; photos adopted from Seilacher et al. (2005) and Mángano and Buatois (2020). Typical field photos of the vertical and subvertical dwelling burrows *Skolithos* **(C)**, two opening of U-shaped *Arenicolites* **(D)**, and *Diplocraterion* **(E)**, which first appeared during Cambrian Stage 2; photos adopted from McIlroy (2017) and our collections from Shiyantou Formation, Yunan, China, and Hardeberga Formation, Bornholm, Denmark (Cambrian Stage 2). Arthropod trackway *Diplichnites* **(F)** from Cambrian Stage 2 (Pandey et al. 2014); and putative farming traces *Paleodictyon* cf. *imperfectum* **(G)** from the Goldenville Group, Nova Scotia, Canada (Pickerill and Keppie 1981). Scale bars, 1 cm.

come onto the stage by the first round of overall divergence of behaviors.

Functional Groups

Facilitated by the evolution of more sophisticated sensory, cognitive and locomotory capabilities during the Ediacaran–Cambrian, early animals began to explore deeper tiers within the substrate. Based on their impacts on sedimentary ecosystems, these organisms can be classified into six categories (Francois et al. 2002; Solan and Wigham 2005): (1) epifaunal bioturbators living on substrates without penetrating the sediment–water interface (e.g., arthropods and gastropods), which can produce surficial traces like *Rusophycus*, *Cruziana*, and *Curvolithus*; (2) surficial modifiers living within the uppermost layers of the sediments (e.g., some meiofauna), which tend to create shallow horizontal burrows like *Gordia*; (3) biodiffusive bioturbators disturbing deeper mixed layers (e.g., bivalves), which leave deep horizontal or plug-shaped burrows, such as *Psammichnites*; (4) regenerators creating semipermanent vertical/oblique burrows that serve to extend the water column downward (e.g., crustaceans and *Skolithos*); (5) conveyors transporting sediment particles between the surface and the bottom of a vertical or oblique burrow (e.g., polychaetes), which produce traces that tend to have backfills and spreites, like *Rhizocorallium* and *Diplocraterion*; (6) gallery biodiffusors creating interconnected burrow systems with one or more openings to the surface (e.g., polychaetes), like *Trichophycus and Paleodictyon*.

Using the data in Table 3, we calculated dissimilarities and balance indices for these different functional groups. The number of

https://doi.org/10.1017/pab.2024.40 Published online by Cambridge University Press

occurrences of traces with two different interpretations (e.g., *Gordia* produced by meiofauna [e.g., foraminifera] as a surficial modifier or produced by small arthropods as epifaunal bioturbators) were halved for each functional group, similar to equation (16). The results are shown in Figure 7.

The dissimilarities of epifaunal bioturbators (E) and surficial modifiers (SM) show very similar profiles, with dissimilarity reaching a peak at the boundary between the Ediacaran and the Cambrian, before decreasing steadily through the Cambrian (Fig. 7A). This indicates these two functional groups were the dominant bioengineers during the Ediacaran and earliest Cambrian, at which time early mobile animals were largely restricted to the surface of the substrate and the topmost layers of sediment. To be precise, the dissimilarities of traces left by epifaunal bioturbators over different intervals are all larger than those of surficial modifying traces that penetrate shallowly into the substrates. This means there are even more animals living on the substrate surfaces compared with those in shallow sedimentary layers. Interestingly, the profile of epifaunal bioengineers' evolutionary dissimilarities also shows common features with those of pascichnia in Figure 5, indicating that the main approach through which these epifaunal benthos transformed the substrate during the Ediacaran was grazing, and these bioengineers were important components of the FDE, as shown by the evident origination components shown in Figure 7C. Following the Fortunian, as the matground became more disturbed (Mángano and Buatois 2020), the diversification rate of grazing epifaunal animals (and their traces) decreased.

The traces left by regenerators (R) and conveyors (C), which produced vertical, subvertical, or oblique burrows, reached peaks in dissimilarity at the boundary between the Fortunian and Cambrian Stage 2 (Fig. 7A), corresponding to the profile of domichnia (Fig. 5), which are also dominated by vertical burrows. This again highlights that although the exploration of deeper tiers by animals started in the Fortunian, this became more prominent (as evidenced by the high balance index for origination and extinction between the Fortunian and Cambrian Stage 2; see Fig. 7C) during the second stage of the Cambrian (Buatois et al. 2020), perhaps due to greater maneuverability, presence of a mineralized exoskeleton, and/or predation pressure in these early animals. These regenerators and conveyors extended the lower boundary of the water column to the burrow bottom, thereby enhancing nutrient exchange between the water column and the substrate. As a result, they can be seen as pioneering ecosystem engineers that transformed the substrate from a two-dimensional stabilized matground into a three-dimensional heterogeneous mixground, ushering in the AR (Buatois et al. 2014).

Biodiffusive bioturbators (B) and gallery biodiffusors (G) diversified slightly later in the Cambrian and peaked in ichnodissimilarity at the interface between Cambrian Stages 2 and 3 (Fig. 7A), showing certain similarities to agrichnia (Fig. 5). This change in the dissimilarity of traces produced by gallery biodiffusors is a result of the appearance of new ichnotaxa (Bauplans or behaviors), evidenced by the high origination of gallery biodiffusors after Cambrian Stage 3 (Fig. 7C), while the peak of traces left by biodiffusive bioturbators was the result of both origination in Cambrian Stage 2 and increased occurrences of existing taxa (mainly those that originated in Stage 2; shown in Fig. 7B,C). In many cases, these tracemakers would have had to simultaneously move their bodies forward while also removing sediments, and hence would likely have required more advanced mobility, maneuverability, sensibility, and even cognition (especially for burrow systems). These biodiffusors would have further enhanced the mixing rate and nutrient exchange within the substrate by creating complex burrow systems. The existence of a better-developed sedimentary mixed layer would have reduced the chances of preserving surficial and semi-infaunal trace fossils (Tarhan 2018). This is also one possible explanation for the persistent decrease in the dissimilarity of the traces left by epifaunal bioturbators and surficial modifiers after the Fortunian (Fig. 7A), when regenerators, conveyors, biodiffusive bioturbators, and gallery biodiffusors started to flourish.

The patterns of dissimilarity in functional groups across the Ediacaran and the Cambrian (Fig. 7A) indicate a progressive and expansive exploration of substrates or niches through this interval, from surface, shallow-surface, and vertical burrows to burrow systems, with progressively stronger capability to maneuver in sediments. However, balance indices (Fig. 7B,C) generally show that all the functional groups underwent a similar two-phase diversification of origination and expansion, which is consistent with the full ichnological dataset (Fig. 4B). The first peak occurred at the Ediacaran/Cambrian boundary, when the earliest complex animals underwent phylum-level diversification. The number of occurrences for some functional groups (e.g.,

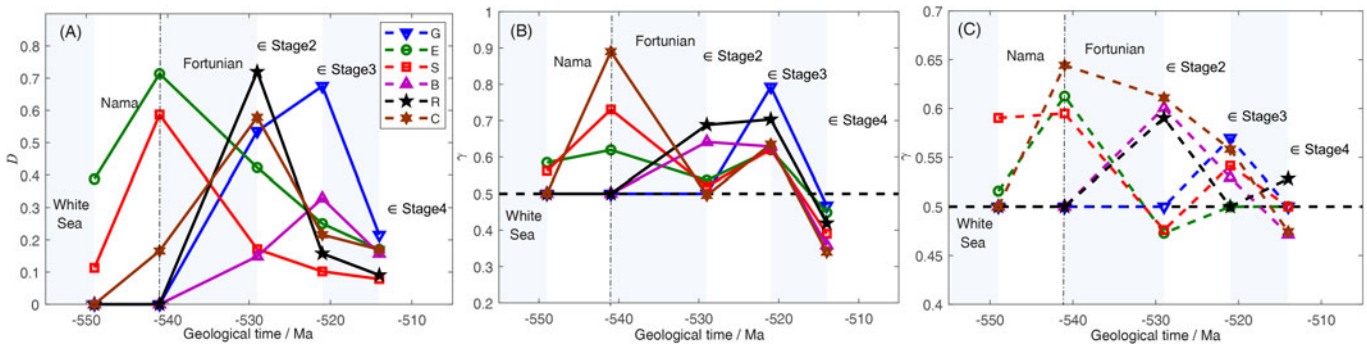


Figure 7. Exploration of function groups and niches across the Ediacaran–Cambrian interval. E, epifaunal bioturbators; SM, surficial modifiers; B, biodiffusive bioturbators; R, regenerators; C, conveyors; G, gallery biodiffusors. **A,** Dissimilarity: epifaunal bioturbators and surficial modifiers experienced massive divergence at Ediacaran/Cambrian boundary, regenerators and conveyors significantly increased after Fortunian, while gallery biodiffusors and biodiffusive bioturbator reached their peak at the interface between Cambrian Stages 2 and 3. **B,** Balance index for occurrences: almost all functional groups experienced a two-peak increase in diversity and occurrences at the Ediacaran–Cambrian interface and the interface between Cambrian Stages 2 and 3. **C,** Balance index for origination and extinction: shallow niches experienced origination earlier than deeper niches, and a small origination happened during Cambrian Stage 3.

https://doi.org/10.1017/pab.2024.40 Published online by Cambridge University Press

conveyors) were not particularly high at this time, despite the evidence for considerable innovation. The second peak occurred at the boundary between Cambrian Stages 2 and 3, corresponding to global genus-level diversification (Na and Kiessling 2015), with similar body plans and behaviors causing an increased abundance within the same ichnogenus. By Cambrian Stage 4, animals from different functional groups were all experiencing more loss of occurrences or even taxa, which may have been the result of local extinctions of stem-group taxa (Zhuravlev and Wood 2018) and limited possibilities for innovations.

Shallow- and Deep-Marine Environments

In addition to the aforementioned analyses of the diversification of traces, behaviors, and functional groups, the proposed measure of ichnodissimilarity can also be used to compare traces from different environments. As illustrated in Figure 8, dissimilarity, the balance index for occurrences, and the balance index for origination and extinction can be used to determine differences between successive stages across Ediacaran and Cambrian deep/shallow seas, as well as the beta diversity between deep and shallow seas during the same stage.

Figure 8 shows that all the dissimilarities and more than half of the balance indices of traces across Ediacaran and Cambrian shallow-sea facies (top, rippled) were higher than those of deep-sea facies (bottom, dotted). This suggests that more substantial evolutionary changes in mobile animals occurred in shallow-marine settings during this interval (Gougeon et al. 2018b), both in terms of their abundance and origination. This is coincident with the diversification of major animal groups and ethological innovation from the trace fossil record: for example, the appearance of the resting trace *Rusophycus* in shallow-marine settings, which is thought to have been produced by trilobites; the vertical tube burrows in nearshore high-energy facies produced by dwelling behaviors.

Ediacaran and Cambrian deep-marine environments had relatively low dissimilarities and abundance (Fig. 8) across time intervals, with the trace fossils mostly simple horizontal locomotory/grazing traces like *Helminthoidichnites* or *Helminthopsis*, as well as the resting or dwelling traces *Bergaueria*, which are thought to have been made by sea anemones (as shown in Table 3). These simple traces, which mostly are indicative of grazing feeding strategies, imply the persistence of a matground ecology from the Ediacaran into the earliest part of the Phanerozoic (Buatois and Mángano 2003; Buatois et al. 2014). This discrepancy in the rate of evolution of animals in shallow- and deep-marine environments reflected by differences in their dissimilarity and the balance index for origination and extinction could be a result of the higher energy conditions in shallow seas: turbulent flow in neritic regions accelerated water, nutrient, and oxygen exchange between the water column and the sediment and thus would have increased the heterogeneity and oxygen content of the substrate (Li et al. 2020). This heterogeneous mixground may have driven benthic animals to develop stronger cognition, detectability, and maneuverability capabilities to survive. And in turn, the bioturbation caused by these more complex behaviors could have further heterogenized the substrate (Gougeon et al. 2018b), promoting the evolution of functional morphology and ethology (i.e., the "savannah" hypothesis for early bilaterian evolution) (Budd and Jensen 2015; Mitchell et al. 2020). All these processes would have been facilitated by the abundance of oxygen and warmer temperature in shallow-marine settings during this time interval. Additionally, the decayed dead metazoans and the organic matter brought by the tides and transgression in the late Ediacaran and early Cambrian would ultimately rejoin this active carbon cycle (Herringshaw et al. 2017) in turbulent shallow-marine settings. Such changes in carbon availability and organism–environment coevolution culminated in a major evolutionary radiation of mobile animals in shallow-marine settings during the Cambrian. Traces (and the tracemakers) that were mainly found in deep-marine settings in later geological periods, like *Paleodictyon*, *Protovirgularia*, *Zoophycos*, *Helminthoida*, and *Nereites*, are thought to have actually originated and migrated from Cambrian shallow-marine environments (Crimes and Fedonkin 1994; Zhang et al. 2015; Hammersburg et al. 2018).

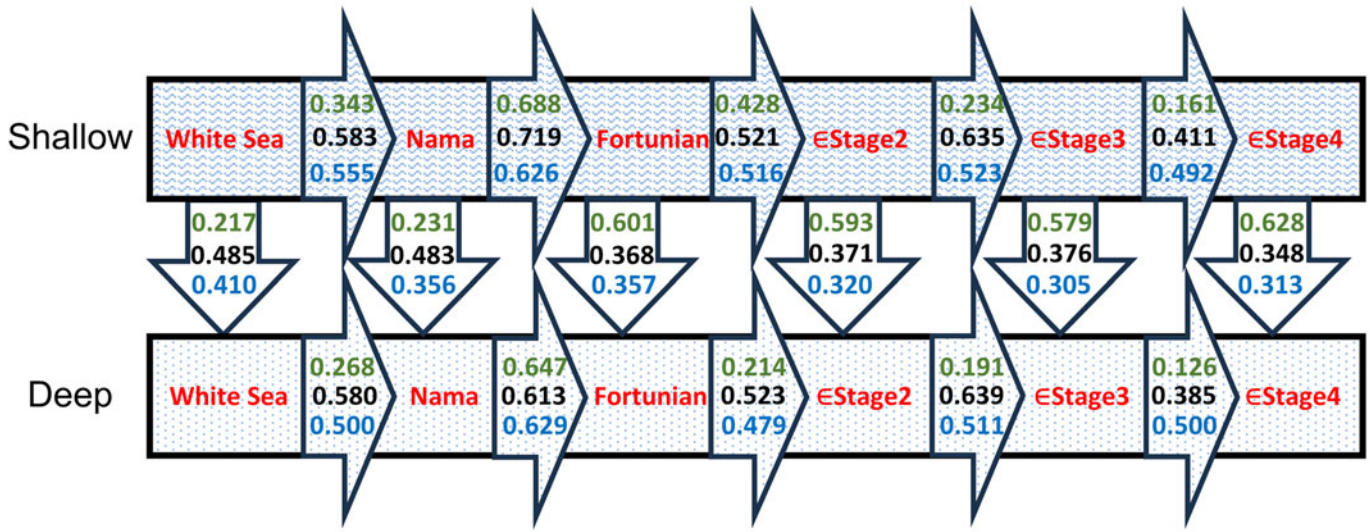


Figure 8. Ichnological dissimilarity (green values), balance index for occurrences (black values), and balance index for origination and extinction (blue values) in different environments across the Ediacaran–Cambrian interval. The dissimilarities between geological intervals at shallow-marine settings (rippled background) is higher than those of the deep-marine settings (dotted background), with slightly higher balance indices especially at the Ediacaran/Cambrian transition. Dissimilarity (beta diversity) is low between contemporaneous shallow- and deep-marine environments during the Ediacaran, while higher during the Cambrian, but shallow-marine settings always has more abundance and taxa than deep-marine settings.

https://doi.org/10.1017/pab.2024.40 Published online by Cambridge University Press

Dissimilarities and balance indices of both shallow- and deep-marine environments show similar profiles to the overall trend for the trace fossil record (Fig. 4), with a maximum dissimilarity at the Fortunian linked to the origination of taxa with fairish abundance, and a smaller second peak in balance indices at Cambrian Stage 3 due to increased abundance of existing taxa, with limited originations. The loss of taxa and abundance exceeded the gains later in Cambrian Stage 4.

Dissimilarity (or beta diversity) between contemporaneous shallow- and deep-marine benthic communities (Fig. 8, middle) has lower value for the Ediacaran period (0.217 and 0.231) compared with the Cambrian (~0.6). This implies a greater (triple) niche overlap between shallow- and deep-marine mobile communities during the Ediacaran (Mángano and Buatois 2016), which could indicate that shallow- and deep-marine ecosystems were relatively similar at this time, or the animals had not yet experienced evident divergence across bathymetry. However, as the substrate became heterogenized due to bioturbation and high-energy flow, especially in the neritic region, stronger niche partitioning occurred, and dissimilarity between shallow- and deep-marine mobile communities increased to 0.6 during the Cambrian. Ecological specialization during this period is also observed when looking at the body fossil record (Eden et al. 2022).

All the balance indices between contemporary shallow and marine seas, as shown in the middle lines in Figure 8, are less than 0.5. This suggests that, in addition to overlapping niches/ichnogenera, there were more ichnogenera existing in shallow-marine environments than in deep-marine ones across the Ediacaran and Cambrian. Particularly in the Ediacaran, all the trace fossils in deep-marine settings can also be found in shallow-marine settings. This suggest that complex mobile animals (i.e., bilaterians) might have evolved in shallow-marine environments (e.g., traces from Dengying Formation; Chen et al. 2018), whereas earlier sessile forms (e.g., frondose representatives of the Ediacara biota) originated in deeper, cold, and stenothermal environments (Boag et al. 2018; Darroch et al. 2021; Turk et al. 2022), with higher intersite beta diversity (Finnegan et al. 2019).

Conclusions

The measure for estimating dissimilarity proposed herein has great potential for estimating differences between communities across environmental gradients (e.g., shallow to deep marine) and geological time spans. Using this approach, we were able to quantify trace fossil diversity across major evolutionary events during the Ediacaran–Cambrian.

The results demonstrate that there was a sudden increase in both the diversity and frequency of occurrences of traces at the beginning of the Phanerozoic, associated with the CIR during the Fortunian. Peaks in ichnodissimilarity and the high balance indices during this period signal the onset of the FDE.

The evolution of more complex animal behaviors and the exploration of deeper tiers/broader territories were rooted in the Fortunian, but prospered later in Cambrian Stage 2. This ethological diversification and the establishment of conveyors and regenerators was characterized by the appearance of new and more efficient feeding strategies and deep vertical burrow systems with passive and active infills. This also served to shift the dominant mode of bioturbation from diffusion to advection of solid sediment/nutrient particles (but this was not necessarily true for oxygen; e.g., see Cribb et al. 2023), which may have been associated with an increase in the extent of the mixed layer. These novel three-dimensional organism–substrate interactions became dominant in Cambrian Stage 2, marked the onset of the AR, and paved the way for the later, more vigorous diversification of animal crown-groups and the Cambrian substrate revolution. Many tracemakers also experienced a second, but lower, peak in Cambrian Stage 3, mainly due to increases in abundance, but also with limited diversification. This corresponds with the expanded global genus-level body fossil record, where Bauplans and behaviors are more conserved and could lead to similar trace morphologies. But later on during Stage 4, a loss of abundance or even extinction was observed. The lowest ichnodissimilarity at Cambrian Stage 4 is also believed to be a result of fully exploited living strategies (e.g., feeding, moving) and niches. The origination (Fortunian)–expansion (Cambrian Stage 3) two-phase pattern is identified through analyses.

Furthermore, we find evidence for asynchrony of evolution in shallow- and deep-marine environments, indicating a more rapid evolutionary radiation in benthic regions during the Ediacaran–Cambrian interval. The lower dissimilarity of trace records during the Ediacaran also indicates an overlapped niche, which then became more specialized during Cambrian explosion.

Our measure of ichnodissimilarity could also be used to analyze diverse aspects of trace fossil diversity and abundance, such as the evolution of architectural designs, which might provide a more objective insight into the divergence of organismal body plan and mobility. Vectorizing trace fossil data could also help reveal hierarchical relationships by assigning different dimensions or positions to taxonomic units, and could be seamlessly integrated into various multivariate statistical techniques such as ordination methods, multivariate regression, and dimensionality reduction, as well as deep learning approaches. We therefore believe that the proposed metrics represent powerful tools to investigate how evolution took place during critical events in Earth's history. This could provide new insights into how body plans, behaviors, and niches diversified in different environments during the emergence of complex animal life. Methodologically, the proposed metrics are also applicable to body fossil and extant animal databases.

Acknowledgments. This work was supported by funding from the Royal Society and the K.C. Wong Education Foundation to Z.W. (NIF R1 221871). We thank A. Bush, A. Cribb, and the anonymous reviewers for helpful comments on an earlier version of this article.

Competing Interest. The authors declare no competing interests.

Literature Cited

Alpert, S. 1973. Bergaueria Prantl (Cambrian and Ordovician), a probable actinian trace fossil. *Journal of Paleontology* **47**:919–924.

Antcliffe, J. B, R. H. T. Callow, and M. D. Brasier. 2014. Giving the early fossil record of sponges a squeeze. *Biological Reviews of the Cambridge Philosophical Society* **89**:972–1004.

Artime, O., and M. De Domenico. 2022. From the origin of life to pandemics: emergent phenomena in complex systems. *Philosophical Transactions of the Royal Society A* **380**:20200410.

Beck, J., J. D. Holloway, W. Schwanghart, and D. Orme. 2013. Undersampling and the measurement of beta diversity. *Methods in Ecology and Evolution* **4**:370–382.

Boag, T. H., R. G. Stockey, L. E. Elder, P. M. Hull, and E. A. Sperling. 2018. Oxygen, temperature and the deep-marine stenothermal cradle of Ediacaran evolution. *Proceedings of the Royal Society B* **285**:20181724.

Bottjer, D. J., J. W. Hagadorn, and S. Q. Dornbos. 2000. The Cambrian Substrate evolution. *GSA Today* **10**:1–8.

https://doi.org/10.1017/pab.2024.40 Published online by Cambridge University Press

Buatois, L. A. 2018. *Treptichnus pedum* and the Ediacaran–Cambrian boundary: significance and caveats. *Geological Magazine* **155**:174–180.

Buatois, L. A., and M. G. Mángano. 2003. Early colonization of the deep sea: ichnologic evidence of deep-marine benthic ecology from the Early Cambrian of northwest Argentina. *Palaios* **18**:572–581.

Buatois, L. A., and M. G. Mángano. 2004. Terminal Proterozoic–Early Cambrian ecosystems: ichnology of the Puncoviscana Formation, northwest Argentina. *Fossils and Strata* **51**:1–16.

Buatois, L. A., and M. G. Mángano. 2016. Recurrent patterns and processes: the significance of ichnology in evolutionary paleoecology. Pp. 449–473 *in* M. G. Mángano and L. A. Buatois, eds. *The trace-fossil record of major evolutionary events*. Topics in Geobiology. Springer, Dordrecht, Netherlands.

Buatois, L. A., and M. G. Mángano. 2018. The other biodiversity record: innovations in animal-substrate interactions through geologic time. *GSA Today* **28**:4–10.

Buatois, L. A., G. M. Narbonne, M. G. Mángano, N. B. Carmona, and P. Myrow. 2014. Ediacaran matground ecology persisted into the earliest Cambrian. *Nature Communications* **5**:3544.

Buatois, L. A., J. Almond, M. G. Mángano, S. Jensen, and G. J. B. Germs. 2018. Sediment disturbance by Ediacaran bulldozers and the roots of the Cambrian explosion. *Scientific Reports* **8**:4514.

Buatois, L. A., M. G. Mángano, N. J. Minter, K. Zhou, M. Wisshak, M. A. Wilson, and R. A. Olea. 2020. Quantifying ecospace utilization and ecosystem engineering during the early Phanerozoic—the role of bioturbation and bioerosion. *Science Advances* **6**:eabb0618.

Budd, G. E., and S. Jensen. 2015. The origin of the animals and a "Savannah" hypothesis for early bilaterian evolution. *Biological Reviews* **92**:446–73.

Bush, A. M., S.C. Wang, J. L. Payne, and N. A. Heim. 2019. A framework for the integrated analysis of the magnitude, selectivity, and biotic effects of extinction and origination. *Paleobiology* **46**:1–22.

Chao, A., R. L. Chazdon, R. K. Colwell, and T. Shen. 2005. A new statistical approach for assessing similarity of species composition with incidence and abundance data. *Ecology Letters* **8**:148–159.

Cheeyham, A. H., and J. E. Hazel. 1969. Binary (presence-absence) similarity coefficient. *Journal of Paleontology* **43**:1130–1136.

Chen, Z., X. Chen, C. M. Zhou, X. L. Yuan, and S. H. Xiao. 2018. Late Ediacaran trackways produced by bilaterian animals with paired appendages. *Science Advances* **4**:eaao6691.

Chen, Z., C. M. Zhou, X. L. Yuan, and S. H. Xiao. 2019. Death march of a segmented and trilobate bilaterian elucidates early animal evolution. *Nature* **573**:412–415.

Conde, A., and J. Domínguez. 2018. Scaling the chord and Hellinger distances in the range [0,1]: an option to consider. *Journal of Asia-Pacific Biodiversity* **11**:161–166.

Cribb, A. T., C. G. Kenchington, B. Koester, B. M. Gibson, T. H. Boag, R. A. Racicot, H. Mocke, M. Laflamme, and S. A. F. Darroch. 2019. Increase in metazoan ecosystem engineering prior to the Ediacaran–Cambrian boundary in the Nama Group, Namibia. *Royal Society Open Science* **6**:190548.

Cribb, A. T., S. J. van de Velde, W. M. Berelson, D. J. Bottjer, and F. A. Corsetti. 2023. Ediacaran–Cambrian bioturbation did not extensively oxygenate sediments in shallow marine ecosystems. *Geobiology* **21**:435–453.

Crimes, T. P., and M. A. Fedonkin. 1994. Evolution and dispersal of deepsea traces. *Palaios* **9**:74–83.

Curran, H. A., and B. Glumac. 2022. *Dactyloidites ottoi* (Geinitz, 1849) in Bahamian Pleistocene carbonates: a shallowest-marine indicator. *Geological Society of London Special Publication* **522**:35–35.

Darroch, S. A. F., A. T. Cribb, L. A. Buatois, G. J. B. Germs, C. G. Kenchington, E. F. Smith, H. Mocke, *et al.* 2021. The trace fossil record of the Nama Group, Namibia: exploring the terminal Ediacaran roots of the Cambrian explosion. *Earth-Science Reviews* **212**:103435.

Eden, R., A. Manica, and E. G. Mitchel. 2022. Metacommunity analyses show an increase in ecological specialisation throughout the Ediacaran period. *PLoS Biology* **20**:e3001289.

Erwin, D. H., and S. Tweedt. 2012. Ecological drivers of the Ediacaran–Cambrian diversification of Metazoa. *Evolutionary Ecology* **26**:417–33.

Evans, S. D., C. Tu, A. Rizzo, R. L. Surprenant, P. C. Boan, H. McCandless, N. Marshall, S. Xiao, and M. L. Droser. 2022. Environmental drivers of the first major animal extinction across the Ediacaran White Sea-Nama transition. *Proceedings of the National Academy of Sciences USA* **119**: e2207475119.

Fan, J. X., S. Z. Shen, D. H. Erwin, P. M. Sadler, N. MacLeod, Q.-m. Cheng, X.-d. Hou, *et al.* 2020. A high-resolution summary of Cambrian to Early Triassic marine invertebrate biodiversity. *Science* **367**:272–277.

Finnegan, S., G. Gehling, and M. L. Droser. 2019. Unusually variable paleocommunity composition in the oldest metazoan fossil assemblages. *Paleobiology* **45**:235–245.

Francois, F., M. Gerino, G. Stora, J. P. Durbec, and J. C. Poggiale. 2002. A functional approach to sediment reworking by gallery-forming macrobenthic organisms: modelling and application with the polychaete *Nereis diversicolor*. *Marine Ecology Progress Series* **229**:127–136.

Gehling, J. G., B. N. Runnegar, and M. L. Droser. 2014. Scratch traces of large Ediacara bilaterian animals. *Journal of Paleontology* **88**:284–298.

Gougeon, R., D. Néraudeau, M. Dabard, A. Pierson-Wickmann, F. Polette, M. Poujol, and J. Saint-Martin. 2018a. Trace fossils from the Brioverian (Ediacaran–Fortunian) in Brittany (NW France). *Ichnos* **25**:11–24.

Gougeon, R. C., M. G. Mángano, L. A. Buatois, G. M. Narbonne, and B. A. Laing. 2018b. Early Cambrian origin of the shelf sediment mixed layer. *Nature Communications* **9**:1909.

Hammersburg, S. R., S. T. Hasiotis, and R. A. Robison. 2018. Ichnotaxonomy of the Cambrian Spence Shale Member of the Langston Formation, Wellsville Mountains, northern Utah, USA. *Paleontological Contributions* **20**:1–66.

Herringshaw, L. G., R. H. T. Callow, and D. McIlroy. 2017. Engineering the Cambrian explosion: the earliest bioturbators as ecosystem engineers. *Geological Society of London Special Publication* **448**:369–382.

Hofmann, R., M. G. Mángano, O. Elicki, and R. Shinaq. 2012. Paleoecologic and biostratigraphic significance of trace fossils from shallow- to marginal-marine environments from the Middle Cambrian (Stage 5) of Jordan. *Journal of Paleontology* **86**:931–955.

Horn, H. S. 1966. Measurement of "overlap" in comparative ecological studies. *American Naturalist* **100**:419–424.

Hsieh, S., R. E. Plotnick, and A. M. Bush. 2022. The Phanerozoic aftermath of the Cambrian information revolution: sensory and cognitive complexity in marine faunas. *Paleobiology* **48**:397–419.

Ichaso, A., L. A. Buatois, M. G. Mángano, P. Thomas, and D. Marion. 2022. Assessing the expansion of the Cambrian Agronomic Revolution into fan-delta environments. *Scientific Reports* **12**:14431.

James, N. P., D. R. Kobluk, and S. G. Pemberton. 1977. The oldest macroborers: Lower Cambrian of Labrador. *Science* **197**:980–983.

Jensen, S., and K. Mens. 2001. Trace fossils Didymaulichnus cf. tirasesnsis Monomorphichnusisp. from the Estonian Lower Cambrian, with a discussion on the early Cambrian ichnocoenoses of Baltica. *Proceedings of the Estonian Academy of Sciences, Geology* **50**:75–85.

Jost, L. 2007. Partitioning diversity into independent alpha and beta components. *Ecology* **88**:2427–39.

Kaur, R., B. P. Singh, O. N. Bhargava, R. Mikuláš, G. Singla, S. K. Prasad, and S. Stopden. 2021. Ichnology and biostratigraphic significance of Cambrian trace fossils from the lowest stratigraphic level of Kunzam La Formation, Chandra Valley, Lahaul and Spiti, India. *Ichnos* **28**:176–207.

Knaust, D. 2013. The ichnogenus *Rhizocorallium*: classification, trace makers, palaeoenvironments and evolution. *Earth-Science Reviews* **126**:1–47.

Knaust, D. 2018. The ichnogenus *Teichichnus* Seilacher, 1955. *Earth-Science Reviews* **177**:386–403.

Knaust, D., and C. Neumann. 2016. *Asteriacites* von Schlotheim, 1820—the oldest valid ichnogenus name—and other asterozoan-produced trace fossils. *Earth-Science Reviews* **157**:111–120.

Kwak, S. G., and J. H. Kim. 2017. Central limit theorem: the cornerstone of modern statistics. *Korean Journal of Anesthesiolog* **70**:144–156.

Li, C., W. Shi, M. Cheng, C. Jin, and T. J. Algeo. 2020. The redox structure of Ediacaran and early Cambrian oceans and its controls. *Science Bulletin* **65**:2141–2149.

Luo, C., and L. Y. Miao. 2020. A *Horodyskia-Nenoxites*-dominated fossil assemblage from the Ediacaran–Cambrian transition (Liuchapo Formation, Hunan Province): its paleontological implications and stratigraphic potential. *Palaeogeography, Palaeoclimatology, Palaeoecology* **545**:109635.

https://doi.org/10.1017/pab.2024.40 Published online by Cambridge University Press

Mángano, M. G., and L. A. Buatois. 2014. Decoupling. *Proceedings of the Royal Society B* **281**:20140038.

Mángano, M. G., and L. A. Buatois. 2016. *The trace-fossil record of major evolutionary events*. Topics in Geobiology. Springer, Dordrecht, Netherlands.

Mángano, M. G., and L. A. Buatois. 2020. The rise and early evolution of animals: where do we stand from a trace-fossil perspective? *Interface Focus* **10**:20190103.

McArthur, R. H., H. Recher, and M. Cody. 1966. On the relation between habitat selection and species diversity. *American Naturalist* **100**:319–332.

McIlroy, D. 2017. Ichnological evidence for the Cambrian explosion in the Ediacaran to Cambrian succession of Tanafjord, Finnmark, northern Norway. *Geological Society of London Special Publication* **448**:351–368.

Mitchell, E. G., S. D. Evans, Z. Chen, and S. Xiao. 2022. A new approach for investigating spatial relationships of ichnofossils: a case study of Ediacaran–Cambrian animal traces. *Paleobiology* **48**:557–575.

Mitchell, E. G, N. Bobkov, N. Bykova, A. Dhungana, A. V. Kolesnikov, I. R. P. Hogarth, A. G. Liu, *et al.* 2020. The influence of environmental setting on the community ecology of Ediacaran organisms. *Interface Focus* **10**:20190109.

Morgan, C. A., C. Henderson, and B. Pratt. 2019. A giant *Protopaleodictyon* from the Middle Cambrian of western Canada. *Ichnos* **26**:216–223.

Na, L., and W. Kiessling. 2015. Diversity partitioning during the Cambrian radiation. *Proceedings of the National Academy of Sciences USA* **112**:4702–4706.

Orloci, L. 1967. An agglomerative method for classification of plant communities. *Journal of Ecology* **55**:193–206.

Pandey, D. K., A. Uchman, V. Kumar, and R. S. Shekhawat. 2014. Cambrian trace fossils of the Cruziana ichnofacies from the Bikaner-Nagaur Basin, north western Indian Craton. *Journal of Asian Earth Sciences* **81**:129–141.

Peters, J. A. 1968. A computer program for calculating degree of biogeographical resemblance between areas. *Systematic Zoology* **17**:64–69.

Pickerill, R. K., and J. D. Keppie. 1981. Observations on the ichnology of the Meguma Group (?Cambro–Ordovician) of Nova Scotia. *Maritime Sediments and Atlantic Geology* **17**:130–138.

Plotnick, R. E., S. Q. Dornbos, and J. Y. Chen. 2010. Information landscapes and sensory ecology of the Cambrian Radiation. *Paleobiology* **36**:303–17.

Ricotta, C. 2017. Of beta diversity, variance, evenness, and dissimilarity. *Ecology and Evolution* **7**:4835–43.

Roy, A. B., and R. Purohit. 2018. Palaeozoic geological history. Pp. 635–646. *In* R. Purohit and A. B. Roy, eds. *Indian Shield: Precambrian evolution and Phanerozoic reconstitution*. Elsevier, India.

Seilacher, A., and J. W. Hagadorn. 2010. Early molluscan evolution: evidence from the trace fossil record. *Palaios* **25**:565–575.

Seilacher, A., and F. Pflüger. 1994. From biomats to benthic agriculture: a biohistoric revolution. Pp. 97–105 *in* W. E. Krumbein, D. M. Peterson, and L. J. Stal, eds. *Biostabilization of sediments*. Bibliotheks-und Informationssystem der Carl von Ossietzky Universität Oldenburg, Oldenburg, Germany.

Seilacher, A., L. A. Buatois, and M. G. Mángano. 2005. Trace fossils in the Ediacaran–Cambrian transition: behavior diversification, ecological turnover and environmental shift. *Palaeogeography, Palaeoclimatology, Palaeoecology* **227**:323–356.

Sepkoski, J. J., Jr. 1998. Rates of speciation in the fossil record. *Philosophical Transactions of the Royal Society B* **353**:315–326.

Solan, M., and B. D. Wigham. 2005. Biogenic particle reworking and bacterial-invertebrate interactions in marine sediments. *In* E. Kristensen, R. R. Haese, and J. E. Kostka, eds. *Macro- and micro-organisms in marine sediments. Coastal and Estuarine Studies* **60**:105–204. American Geophysical Union, Washington, D.C.

Tarhan, L. G. 2018. The early Paleozoic development of bioturbation—evolutionary and geobiological consequences. *Earth-Science Reviews* **178**:177–207.

Turk, K. A., K. M. Maloney, M. Laflamme, and S. A. F. Darroch. 2022. Paleontology and ichnology of the late Ediacaran Nasep–Huns transition (Nama Group, southern Namibia). *Journal of Paleontology* **96**:753–769.

Wang, Z. K., and I. Rahman. 2023. Quantitative ichnology: a novel framework to determine the producers of locomotory trace fossils—the ichnogenus *Gordia* as a case study. *Palaeontology* **66**:e12686.

Webby, B. D. 1970. Late Precambrian trace fossils from New South Wales. *Lethaia* **3**:79–109.

Whittaker, R. H. 1960. Vegetation of the Siskiyou Mountains, Oregon and California. *Ecological Monographs* **30**:279–338.

Wilson, T. L., A. P. Rayburn, and Jr T. C. Edwards. 2012. Spatial ecology of refuge selection by an herbivore under risk of predation. *Ecosphere* **3**:1–18.

Zamora, S., B. Deline, J. J Álvaro, and I. A. Rahman. 2017. The Cambrian Substrate Revolution and the early evolution of attachment in suspension-feeding echinoderms. *Earth-Science Reviews* **171**:478–491.

Zhang, X. L., and D. G. Shu. 2021. Current understanding on the Cambrian Explosion: questions and answers. *palZ* **95**:641–660.

Zhang, L. J., R. Y. Fan, and Y. M. Gong. 2015. Zoophycos macroevolution since 541 Ma. *Scientific Reports* **5**:14954.

Zhang, L. J., Y. A. Qi, L. A. Buatois, M. G. Mángano, Y. Meng, D. Li, and R. F. Tang. 2017. The impact of deep-tier burrow systems in sediment mixing and ecosystem engineering in early Cambrian carbonate settings. *Scientific Reports* **7**:45773.

Zhu, M., A. Zhuravlev, R. Wood, F. Zhao, and S. Sokhov. 2017. A deep root for the Cambrian Explosion: implications of new bioand chemostratigraphy from the Siberian PlatformZ. *Geology* **45**:459–462.

Zhuravlev, A., and R. Riding. 2000. *The ecology of the Cambrian radiation*. Columbia University Press, New York.

Zhuravlev, A. Y., and R. A. Wood. 2018. The two phases of the Cambrian Explosion. *Scientific Reports* **8**:16656.

https://doi.org/10.1017/pab.2024.40 Published online by Cambridge University Press